5 DISCUSSION

5.1 OPA1 transcript analysis

5.1.1 Only four OPA1 splice forms are present in mouse tissues

The OPA1 gene is ubiquitously expressed and alternatively spliced into eight different splice variants in humans and in the mouse (Delettre et al., 2001 and 2003). In autosomal dominant optic atrophy patient mutations in OPA1 affect just the optic nerve (Votruba et al., 1998). Such a tissue specific disease phenotype may be caused by the loss of a tissue specific splice variant. Therefore, the aim of this study was to identify tissue specific particularities of OPA1 gene expression. Analysis of mouse brain, heart, liver and kidney tissues did reveal the same set of OPA1 mRNAs to be present in the nervous system as in other tissues. Thus, a disease mechanism based on specific loss of a particular splice form seems to be rather unlikely. Nevertheless, the abundance of individual transcript variants differed significantly for the brain in comparison with the other tissues examined (see below).
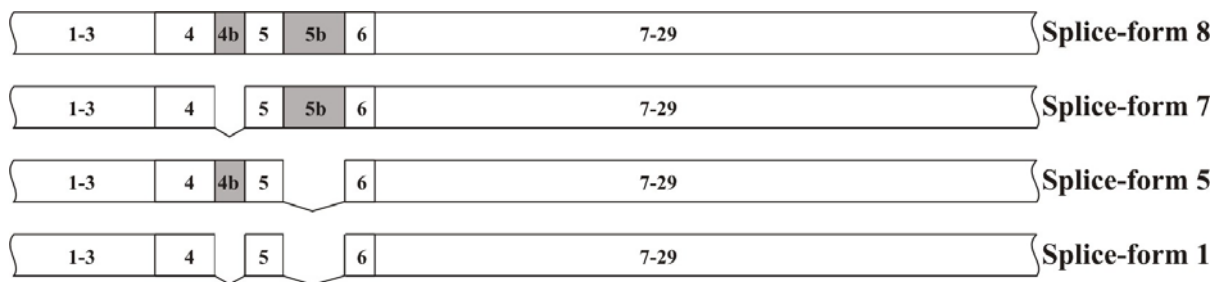

Figure 5.1: OPA1 splice variants found in mouse tissues.
Alternative splicing of exons 4b and 5b (shaded regions) generate four splice variants in mouse.

In contrast to published RT-PCR data, in this work, only four mRNA transcripts, which corresponded to splice variants 1, 5, 7 and 8, were detected. These splice forms were generated by alternative splicing involving exons 4b and 5b (Fig. 5.1). The obtained results did not confirm the involvement of exon 4 of the OPA1 gene in alternative splicing events in the mouse, as was reported earlier (Delettre et al., 2003). Moreover, these data are consistent with the *in silico* data generated by ASePCR v.0.6 (http://genome.ewha.ac.kr/ASePCR/). ASePCR is an efficient web-based application that emulates RT–PCR in various tissues. It estimates the amplicon size for a given primer pair based on the transcript models identified by the reverse e-PCR program of the NCBI. The tissue specificity of each PCR band is deduced from the tissue information of expressed sequence tag (EST) sequences compatible with each transcript structure. The output page shows PCR bands like a gel electrophoresis in various tissues (Kim et al., 2005).

The failure of other groups to notice the exclusive presence of only four splice variants seems to be due to the technical problems. In order to specifically amplify even low abundant transcripts or splice variants with particular exon compositions, four different sets of primers were used in this study (Chapter 4.1). Instead, Delettre and co-workers mentioned only one primer pair flanking the alternatively spliced region that was supposed to amplify fragments from all eight mRNA splice variants in one reaction. Furthermore, they performed agarose gel electrophoresis (AGE) to analyse their amplified products (Delettre et al., 2003). As described in Chapter 4.1, the sequencing results obtained from such agarose bands revealed that these bands did not contain homogeneous fragments of individual splice variants but mixtures of DNA-fragments. Hence, a correlation of the observed bands in AGE with specific OPA1 splice forms based on size is not possible. Importantly in this context, an accurate assertation as to the presence of particular OPA1 splice forms cannot be made. It has to be concluded that AGE is not an appropriate method to determine the identity of OPA1 splice variants.

5.1.2   PAGE is a reliable detection method for OPA1 splice forms

RT-PCR products of OPA1 transcript variants were analysed both on ethidium bromide-stained agarose gels (AGE) and high-resolution silver-stained 5% polyacrylamide gels (PAGE). As discussed in the previous paragraph, AGE did not provide the accurate detection of OPA1 splice variants. Detailed analysis of the RT-PCR products observed in AGE by sequencing indicated the variety of transcripts in each band. These mixtures most likely represent heteroduplexes composed of differently spliced OPA1 cDNAs and were formed during the PCR reaction. Obviously, the loop structures present in DNA hybrids after annealing of different splice variants are thermodynamically tolerated. This may be due to the very small size of exons 4b (54 bp) and 5b (111bp). In contrast to AGE, PAGE produced reliable and reproducible signals of individual OPA1 splice forms (Fig. 4.1 and Fig. 4.4). The same results were also obtained using the primer pair 3-9, or e3-e7 as published by Delettre and colleagues (Table 4.1b). The best separation was achieved in urea-denaturing PAGE, where all bands resulting from double stranded as well as secondary structure forming DNA molecules disappeared. Only the denatured single strands were observed running at their accurate size. This method also ruled out the possibility of different RT-PCR fragments being superimposed thereby provided a better assessment of the expressed transcripts.

5.1.3   The complexity of OPA1 alternative splicing increases during the evolution

OPA1 and its orthologs in different species are encoded by a single nuclear gene. In yeast, *Saccharomyces cerevisiae,* the OPA1 homologous gene, Mgm1, is transcribed as one form of

mRNA, lacking sequences resembling exons 4b and 5b (Olichon et al., 2006). Upon import into mitochondria, the Mgm1 protein is proteolytically cleaved into a long form, l-Mgm1p, and a short form, s-Mgm1p (Herlan et al., 2004). The *Drosophila melanogaster* homologue of *OPA1* is expressed as two mRNA variants generated by alternative splicing of exon 4 while sequences corresponding to exons 4b and 5b are absent. In fish and rat, exons 4b and 5b are present in the genome, but their involvement in splicing has not been investigated. In the mouse, exons 4b and 5b are alternatively spliced, generating four different splice forms. Finally in *Homo sapiens*, the OPA1 gene produces eight mRNA variants through alternative splicing involving exons 4, 4b and 5b (Delettre at al., 2001). It can be concluded that the number of OPA1 gene copies was kept constant while the number of splice variants has increased from evolutionary lower to higher species. Hence, the complexity of OPA1 gene expression has increased during evolution at mRNA level.

Table 5.1: Complexity of OPA1 splicing in different species

Species	Exons present			Exons involved in alternative splicing	Number of mRNA transcripts
	4	4b	5b		
Human	+	+	+	4, 4b, 5b	Eight
Mouse	+	+	+	4b, 5b	Four
Rat	+	+	+	Not known	Not known
Fish	+	+	+	Not known	Not known
Drosophila	+	-	-	4	Two
Yeast	+	-	-	No splicing	One

The post-translational processing of the OPA1 homologue Mgm1 is already detected in yeast (Herlan et al., 2004). In addition, the proteolytic cleavage of OPA1 in the mouse, rat and human was demonstrated. These modifications seem to involve several proteases, further increasing the complexity of regulation at the protein level (Ishihara et al., 2006; Cipolat et al., 2006).

5.2 Identification of various OPA1 protein isoforms

The OPA1 transcript analysis revealed the presence of four different OPA1 splice variants, while at least six different protein isoforms were present on western blots. This indicated that the translated OPA1 proteins undergo post-translational modifications.

Detailed analysis by MS/MS revealed that all OPA1 isoforms contained the C-terminal region starting at amino acid 270. Thus, the differences in migration behaviour in PAGE likely resulted from individual N-termini, starting upstream of amino acid 270 (Fig. 5.2). The N-terminal sequence varies due to exon composition and/or proteolytic cleavage. Two migrating bands at 95-kDa contain OPA1 isoforms 1 and 7. Microsequencing of both forms revealed N-

termini that had resulted from cleavage between amino acids N87/F88. This cleavage site is in agreement with the known conserved motif for the mitochondrial processing peptidase (MPP). Processing by MPP during mitochondrial import leads to maturation of mitochondrial precursors required for mitochondrial biogenesis and function (Luciano and Geli, 1996; Ito, 1999). MPP cleavage leads to sorting of proteins into the mitochondrial inner membrane (Fig. 5.3). This MPP cleavage motif contained within OPA1 exon 2 is present in all OPA1 splice variants and located upstream of the alternatively spliced exons. Therefore, it can be assumed that the two other OPA1 isoforms existing in the mouse, isoforms 5 and 8 undergo the same cleavage upon the import into the mitochondria.
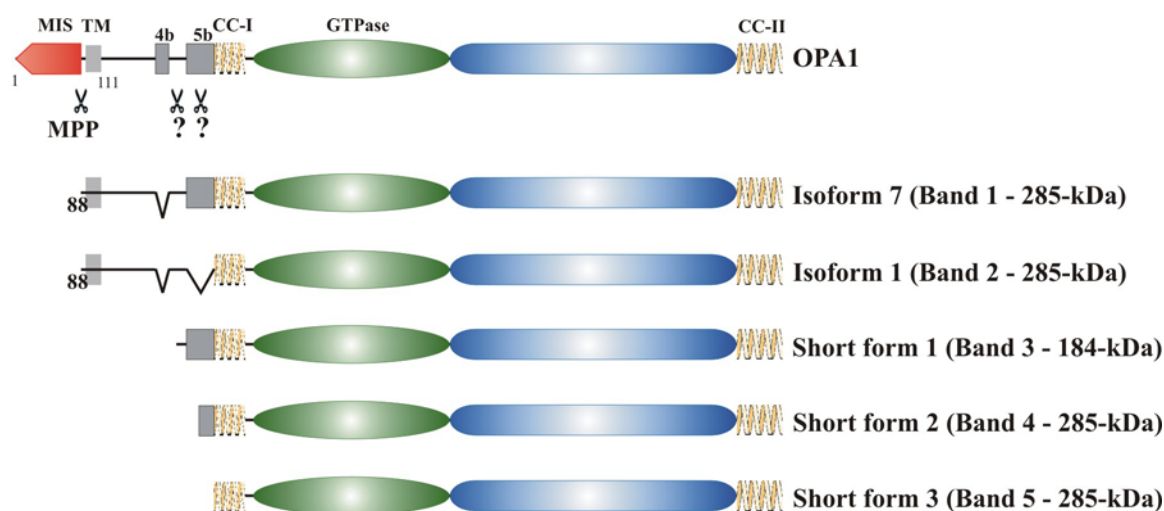

Figure 5.2: OPA1 protein isoforms identified in steady state mitochondria in mouse tissues.
Isoforms 1 and 7 are formed after MPP import cleavage, while short forms are formed by immediate further processing by unknown proteases. OPA1 isoforms form two different high molecular weight complexes of 285-kDa and 184-kDa. MIS -mitochondrial import sequence; TM-transmembrane domain; CC-coiled coil domains; MPP- mitochondrial processing peptidase; domains 4b and 5b are the regions encoded by exons 4b and 5b, respectively.

This finding is in accordance with the most recent report in human cells (Ishihara et al., 2006) and demonstrates that this mechanism is conserved for OPA1 in both humans and mice, and even yeast (Herlan et al., 2004). Earlier studies had proposed different mitochondrial import cleavage sites for human and mouse (Olichon et al., 2002; Misaka et al., 2002). These groups had used reporter assays in order to determine the mitochondrial cleavage site in isolated mitochondria. This *in vitro* situation most likely led to an artifactual cleavage, which is not used under *in vivo* conditions in the mouse and in human cell culture. Moreover, these groups utilized low-resolution gel systems, which did not properly separate the different OPA1 protein isoforms.

N-terminal sequencing of the polypeptides migrating in bands-3 to -5 did not produce reliable sequence data. Examination of the samples by high-resolution 2-D gel electrophoresis

indicated that the protein samples have undergone terminal single amino acid removal (data not shown). These short forms are most likely the resulting products of immediate further processing after MPP import cleavage. Band-3 contained sequences corresponding to exon 5 and 5b, which means, that proteolytic cleavage must have happened in domain 5. In contrast, band-4 contained only the peptides corresponding to exon 5b; hence, isoforms present in this band must have been cleaved in domain 5b. This means, that domain 5b is not necessarily always cleaved. Instead, this cleavage event seems to be regulated by a specific mechanism. Therefore, isoforms present in bands-3 and -4 have to be generated from isoforms 7 and/or 8, both of which contain exon 5b after proteolytic processing by unknown proteases (Fig. 5.3). Isoforms present in band-5 could originate from cleavage in a domain encoded by exon 6 of any isoform of OPA1. Accordingly, isoform 5 could contribute to the formation of band-5. Band-4 was detected as a double band in the western blot analysis. The small size migration difference between the double bands cannot be explained as a result of proteolytic cleavage and may be caused by phosphorylation at amino acid T984 of OPA1 (Brill et al., 2004; Poolak et al., 2006).
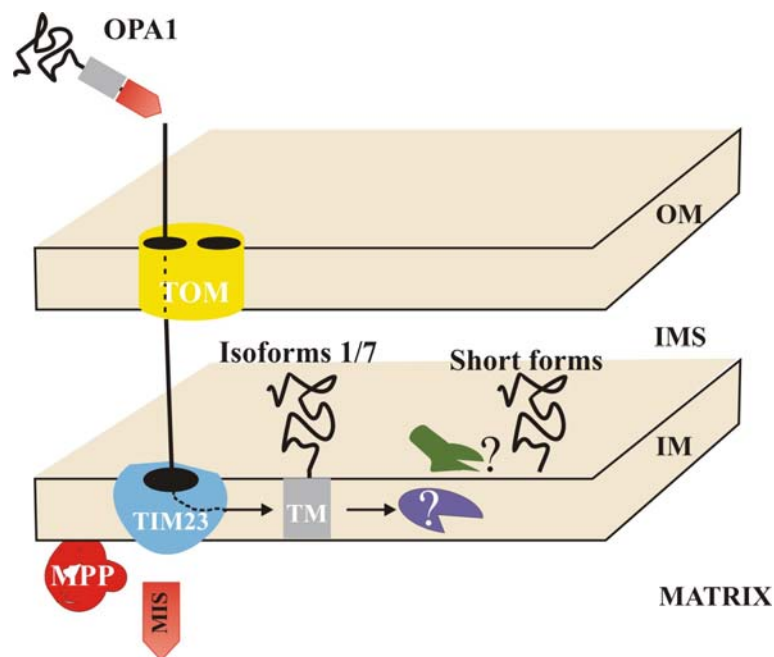

Figure 5.3: Model for OPA1 protein isoforms being processed in the mitochondria.
The TIM23 translocase containing all essential subunits such as Tim23, Tim17, Tim50, Tim14, Tim44, and Ssc1 is shown in transparent blue color. The TOM complex is shown in yellow color. The first transmembrane segment in OPA1 is indicated in gray. The mitochondrial import sequence (in red) is cleaved by MPP present in the matrix. Isoforms 1 and 7 are generated by MPP cleavage and anchored into the inner mitochondrial membrane through the transmembrane domain. The short forms are generated due to subsequent processing after MPP import cleavage by unknown proteases (marked in green and blue). MIS -mitochondrial import sequence; TM -transmembrane domain; MPP -mitochondrial processing peptidase; OM –outer membrane; IMS –inner membrane space; IM –inner membrane.

The overexpression of the two rat OPA1 splice variants 1 and 7 in HeLa cells demonstrated that these variants exist as two (L and S1) and three (L, S1, and S2) proteolytically processed isoforms of distinct lengths, respectively. The MPP cleavage produces the L forms while the second processing at amino acids R212/A213 generates the S1 isoform. The short form S2 of isoform 7 occurred after cleavage around L217/E223. In this report it was argued that the processing of the predominantly expressed isoforms 1 and 7 is sufficient to explain the OPA1 protein pattern (Ishihara et al., 2006). These findings are in accordance with the data obtained in this study; nevertheless, the translation of OPA1 isoforms 5 and 8 in the mouse cannot be excluded.

The proteases involved in processing of OPA1 are unclear. The yeast long form (l-Mgm1) represents the MPP processed form, while the small form (s-Mgm1) is produced after cleavage of l-Mgm1 by the mitochondrial rhomboid protease Pcp1/Rbd1. Herlan and co-workers (2003) proposed that the mammalian homologue of the yeast Pcp1/Rbd1, Presenilin associated rhomboid-like (PARL), (Pellegrini et al., 2001; McQuibban et al., 2003) processes the mammalian OPA1 protein. They predicted cleavage of OPA1 in two hydrophobic segments encoded by exons 4b (aa 193-206) and 5b (aa 227-240). Cipolat and co-workers (2006) co-precipitated OPA1 and PARL and demonstrated that PARL is acting upstream of OPA1 (Cipolat et al., 2006). In contrast, Ishihara and co-workers (2006) demonstrated that in mammalian cells repression or exogenous expression of PARL has no effect on OPA1 processing. Instead, they showed that the m-AAA protease, paraplegin, cleaves OPA1 in mammalian cells. They also proposed a possibility that paraplegin cooperatively regulates OPA1 processing together with PARL or other proteases yet to be identified. The cleavage sites were predicted to reside in sequences encoded by exons 5 and 5b, which is in agreement with my data.

5.2.1 In brain the abundance of OPA1 differs compared to other tissues

The overall amount of RT-PCR product generated from total RNA of brain, liver, heart and kidney tissue did not differ much. Thus, the rate of transcription of the OPA1 gene is comparable for all tissues analysed. A clear variation in abundance for individual splice forms was observed in the brain versus the other tissues. A large predominance of splice form 1 in the brain over splice forms 7 and 5 was noticed, while splice variant 8 was hardly detectable (Table 4.2). This has to be the result of either a different regulation of splicing or mRNA stability of the individual transcript variants. Unpublished northern blot data generated in our lab hint at the involvement of differential polyadenylation in OPA1 post-transcriptional

regulation. Taken together, it can be assumed that the 3'UTR of OPA1 messenger RNAs may have an influence on the level of individual OPA1 splice variants present in a given tissue.

A clear variation in abundance of different OPA1 protein isoforms was noted in all tissues (Fig. 4.9). This indicates that a tissue specific regulation mechanism for OPA1 protein translation exists. Moreover, this study confirmed that OPA1 protein isoform 1 is predominant in the nerve tissues.

Several reports have shown that the expression level of OPA1 transcript variant 1 in the mouse retina is identical to the levels in the brain (Delettre at al., 2001; Kamei et al., 2005), indicating a particular requirement of OPA1 transcript variant 1 in the central nervous system. In addition, overexpression of OPA1 variant 1 protected HeLa cells from undergoing apoptosis after appropriate stimulation (Frezza et al., 2006). Moreover, the mutations identified in autosomal dominant optic atrophy (adOA) patients reside exclusively in exons present in OPA1 splice variant 1. In most cases the mutations result in nonsense mediated decay of the affected transcripts leading to a reduction of the steady-state level of functional transcripts in patient cells (Pesch et al., 2001). Therefore, levels of wildtype OPA1 transcript 1 are always affected in adOA patients. A reduction of the OPA1 transcript variant 1 level in retinal ganglion cells (RGC) in adOA patients may affect protection of RGCs against cell death, thus leading to an increased loss of RGCs.

5.3 Complex forming property of the OPA1 isoforms

5.3.1 Identification of novel OPA1 interaction partners

Proteins interacting with OPA1 have not been described, except for one protein, Ugo1p, in *Saccharomyces cervisiae.* Ugo1p acts as a linker between Mgm1p, in the inner mitochondrial membrane, and Fzo1p in the outer mitochondrial membrane and in this way it provides a scaffold for the assembly of the fusion complex (Wong et al., 2003). Biochemical experiments, undertaken as part of this thesis, show the ability of OPA1 to form high-molecular weight complexes that very likely contain interacting protein partners. However, the Y2H screens, co-immunoprecipitation and size exclusion chromatography did not yield any potential OPA1 interaction partners. Still, it cannot be excluded that OPA1 may associate with other proteins inside mitochondria or in the cytoplasm after it's release from mitochondria during apoptosis (Arnoult et al., 2005; Frezza et al., 2006).

Nevertheless, OPA1 most likely forms stable high molecular weight complexes via self-interaction mediated by the coiled-coil domains.

5.3.2 OPA1 can self associate via its coiled-coil domains

Dynamin-related proteins have the potential to oligomerise into large complexes (Danino and Hinshaw, 2001). For instance, dynamin 1 can tubulate membranes and assembles into oligomers that are necessary to sever membranes (Sweiter and Hinshaw, 1998). Mitofusin 1, a Dynamin located in the outer mitochondrial membrane, forms dimers between two Mitofusin molecules sitting on the surface of two different mitochondria (Koshiba et al., 2004). The Mitofusin dimers are thought to tether mitochondria before they fuse their outer membranes.

OPA1 isoforms form two high-molecular weight protein complexes with apparent molecular masses of 285- and 184-kDa. Both complexes were found in all mouse tissues examined. The higher molecular mass complex of 285-kDa is composed of isoforms 1 and 7, as well as short form 2 and 3, while the smaller complex of 184-kDa is a dimer of short form 1 (Fig. 5.2). This implies that short form 1 differs from all other isoforms in its complex formation behaviour.

These results are not in agreement with those reported earlier (Satoh et al., 2003) that described the existence of only two isoforms of OPA1, 93- and 88-kDa in size. These OPA1 proteins were assigned to two different complexes of approximate sizes of 440 and 150–400 kDa, respectively. Two reasons can explain this discrepancy: 1) The resolution of the SDS-PAGE did not allow for the separation of all 5 different OPA1 isoforms, 2) The usage of Triton X-100 leads to large micelle aggregation, which results in higher apparent values for OPA1 complex sizes. In order to obtain smaller micelles, CHAPS was used as detergent of choice in this work.

Studies by Okamoto and co-workers (1999) indicated that coiled-coil domains are involved in dynamin self-assembly. Coiled-coil domains have an inherent property to self-associate and frequently mediate the formation of complexes between protein molecules (Shin et al., 1999). The N-terminal CC domain (CC-I) of OPA1 forms a strong and stable homo-dimer, while the C-terminal CC domain (CC-IIb) is present in equilibrium between monomer and dimer states. CC-I and CC-II domains do not form any hetero-oligomers. This confirms the specificity of the self-interactions of each OPA1 coiled-coil domain. Furthermore, these data suggest that these coiled coil (CC) domains may support the interaction of the entire OPA1 polypeptides.

The introduction of frame-shift mutations linked to adOA completely abolished the self-association of the CC-IIb peptides. It was also shown that overexpression of a full-length version of OPA1 isoform 1 is able to rescue HeLa cells from entering apoptosis, while a CC-IIb deletion construct (905STOP) is not (Frezza et al., 2006). Together these data suggest that the loss of CC-IIb renders the OPA1 isoform 1 inactive due to its inability to interact and

form oligomers. It might therefore be postulated that CC-IIb alone is capable to mediate OPA1 complex formation of isoform 1. In the size exclusion chromatography experiments, monomers of OPA1 were not observed; instead all OPA1 molecules were involved in stable complex formation. Thus, in order to be in it's an active form; OPA1 protein needs to self-interact what relies on the presence of CC-IIb domain. In adOA patients, the CC-IIb frame-shift mutations will therefore lead to the expression of inactive OPA1 molecules, which will not disturb the wildtype OPA1 molecules. As a result OPA1 will not act in a dominant negative fashion. In such cases, haploinsufficiency in patients with optic atrophy due to loss-of-function of OPA1 at the protein level has to be assumed. In contrast, an alteration of the CC-I domain of OPA1 by mutations or even SNPs has never been reported. This may indicate that any modifications of this domain strongly affect OPA1 function and may be lethal even in the heterozygous condition.
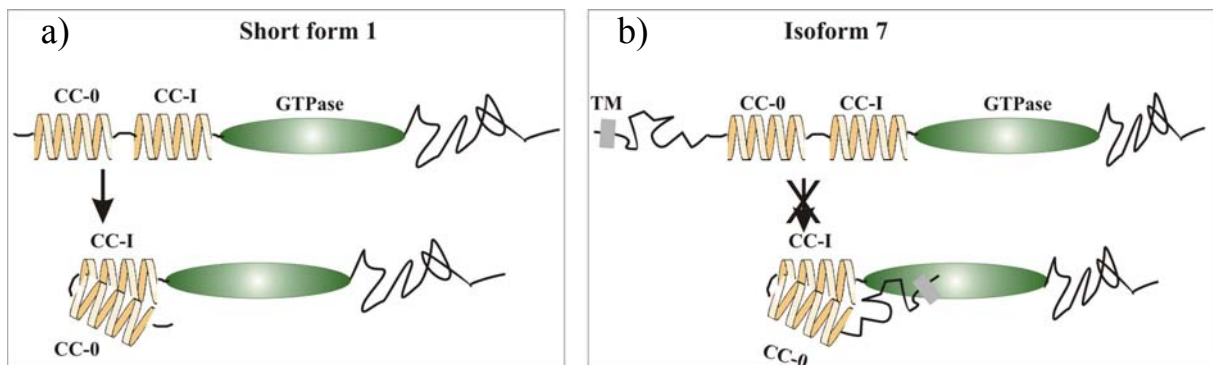

Figure 5.4: Cartoon depicting association of CC-0 and CC-I.
The CC-I domain in short form 1 may be masked by CC-0 (a), while the association is sterically blocked in isoform 7 (b). The CC-I masking in isoform 7 is also hindered due to transmembrane (TM) region that anchors it to the inner mitochondrial membrane.

With the data available to date, it cannot be concluded if the 285-kDa complexes are formed by homo-association of identical isoforms or by hetero-interaction between different OPA1 isoforms. It may even be the case that two or more different complexes exist of roughly similar sizes that all are collected in fraction 19. In contrast, the situation for the small complex is much clearer. Short form 1 forms a low molecular weight homo-dimer, which may be generated due to the trans-interaction of two CC-IIb domains. CC-I potentially could interact *in trans* with a third short form 1 molecule, which would lead to a protein complex of a size larger than ~180 kDa. Since in this work such larger complexes were not observed, an interaction of CC-I seems to be suppressed. Due to alternative splicing, the sequence context around CC-I varies in different isoforms. This provides an option for an individual regulation of binding of OPA1 proteins via CC-I. The N-terminus of short form 1 contains protein stretches encoded by exon 5, 5b and 6. CC-I is encoded by exon 6, but exon 5b is also

translated into a coiled-coil domain (CC-0, a 37 amino acid residue sequence). The binding of CC-0 to CC-I could mask the self-association of CC-I and, thereby restricting the short form 1 to form a dimer via CC-IIb. In support to this hypothesis CC-0 does not self-associate (data not shown). In contrast, isoform 7 (after MPP cleavage) also harbours CC-0, but does not form low molecular weight oligomers. This might be explained by a steric hindrance of CC-0 to interact with CC-I due to the stretch of amino acids present N-terminally to CC-0 (Fig. 5.4). Besides, the transmembrane domain in the isoform 7 is anchored into the inner mitochondrial membrane that obstructs the association of CC-0 and CC-I. However, this hypothesis needs to be validated through additional *in vitro* experiments.

The process of OPA1 oligomerisation and the existence of different OPA1 complexes have hardly been investigated. In one recent study, it was shown that oligomers of OPA1 appear to be involved in the regulation of cytochrome c release during apoptosis (Frezza et al., 2006). A model was proposed in which a hetero-trimer consisting of two membrane-bound and one soluble form of OPA1 maintains tightness of cristae junctions. Upon disruption of this complex by cBID, inner mitochondrial membranes were remodelled preceding the complete release of cytochrome c into the cytoplasm. As membrane-bound forms, only the uncleaved forms of isoform 1 or 7 can be considered, because only these were found to be strongly associated with the mitochondrial membranes. The soluble third component of the complex must be the short form 2 or 3, since short form 1 builds up an independent complex. A detailed investigation comparing OPA1 complexes in mitochondria before and after cytochrome c release, while simultaneously blocking the full execution of apoptosis, should give further insights into this question. Moreover, OPA1 null cells, transfected with individual isoforms will allow the determination of complex forming potential of different OPA1 isoforms.

5.3.3 *Membrane topology of the OPA1 isoforms*

Isoforms 1 and 7 only, contain the predicted transmembrane (TM) domain at the N-terminus after the MPP cleavage in the mouse mitochondria (Fig. 5.2). Although OPA1 protein isoforms 1 and 7 are assumed to possess a transmembrane type I topology, a significant fraction of these proteins was extracted from the inner membrane by alkaline treatment. The partial extraction of these isoforms could be due to the relatively weak hydrophobicity of the putative TM that fails to firmly anchor them to the inner membrane. The mitochondrial apoptosis-inducing factor (AIF), a type I inner membrane protein with bulk of the C-terminal segment exposed to the mitochondrial inter-membrane space, displayed a similar behaviour (Ishihara et al., 2006; Otera et al., 2005). Most of the short forms were extracted into the

soluble fraction indicating absence of any TM domain in these forms. The short forms are proteolytically processed further towards C-terminus then isoforms 1 and 7, and hence lost this TM domain. However, a very small fraction of these short forms still remained in the membrane fraction, which could be attributed, either, to their strong hydrophobic coiled-coil domain interactions with the membrane-associated forms of OPA1 or a possible second weak hydrophobic segment as predicted for the regions encoded by exons 4b and 5b of OPA1 (Herlan et al., 2004). Our results are in complete agreement with the most recent reports, which state that the short isoforms could be extracted from mitochondria with detergent-free buffer with higher efficiency than the larger forms, suggesting that the latter ones are integral membrane protein isoforms, and the short ones are only peripherally attached to the membrane (Duvezin-Caubet et al., 2006).

Mgm1 has two hydrophobic segments at the N-terminus and is anchored to the inner membrane through the first hydrophobic segment (TM1). Processing by Pcp1/Rbd1 occurs only when the cleavage site in the second hydrophobic segment localized in the intermembrane space reaches the inner membrane, what is driven by matrix ATP and the pre-protein import motor (Herlan et al., 2004). In this case, TM1 functions as a stop-transfer sequence and the hydrophobicity of TM1 underlies the processing efficiency; TM1 with increased hydrophobicity strongly inhibits the processing. However, the OPA1 processing was not inhibited by increment of TM hydrophobicity though it increased the membrane anchoring efficiency of OPA1 as assessed by alkaline treatment (Ishihara et al., 2006). This observation might reflect an inherent difference in the mechanism of controlling the cleavage and ratios of OPA1 and Mgm1 isoforms between mammalian and yeast mitochondria, respectively. Taken together this clearly suggests that OPA1 processing is driven by a mechanism distinct from that of yeast Mgm1.

5.4   Conclusions and future perspectives

The complexity of OPA1 gene expression increased during evolution, additional splice forms of OPA1 were generated by alternative splicing.

1. What is the function of these individual OPA1 splice forms?
2. Why are the additional OPA1 splice forms necessary?

OPA1 null mouse embryonic fibroblast cell line available in our lab is the best tool to answer these questions. Generating permanent cell lines expressing each of the splice variants would identify the function of individual splice forms by studying their ability to rescue the impaired mitochondrial morphology.

While the overall level of OPA1 gene transcription seems to be constant in different tissues, the individual brain expression level of the four splice variants in the mouse differs from other tissues, indicating tissue specific post-transcriptional regulatory mechanisms.

1. Why does the mouse brain require different amounts of OPA1 isoform 1 than the other tissues?
2. How is the predominant expression of isoform 1 in the brain regulated?

The regulation of OPA1 protein expression may not be due to splicing, but could result from mRNA stability and transcriptional repression, which requires further investigation.

Six OPA1 protein isoforms exist and likely are processed by MPP upon mitochondrial import. This cleavage sorts the proteins into the mitochondrial inner membrane. Furthermore, the post-import processing occurs after the mitochondrial import.

1. Why is the post-MPP processing necessary?
2. What are the processing enzymes?
3. What are their cleavage sites?

The processing events can be studied in OPA1 null cells by overexpressing individual isoforms. Additionally, the role of exons 4, 4b and 5b, in the cleavage mechanisms can be determined.

OPA1 exists as two different complexes (having molecular weight of 184- and 285-kDa), which are formed due to the self-interaction of the coiled coil domains present in OPA1 isoforms.

1. What is the composition of 285-kDa complexes?
2. What is the function of these two complexes?

The studies on the composition of OPA1 complexes can be performed in OPA1 null cells, wherein the contribution of each OPA1 isoform can be evaluated.